

## PROBABILISTIC MODELS FOR THE ASSESSMENT OF CYCLIC SOIL STRAINING IN FINE-GRAINED SOILS

H. Tolga BILGE<sup>1</sup>, K. Onder CETIN<sup>2</sup>

### ABSTRACT

A maximum likelihood framework for probabilistic assessment of post-cyclic soil strains in fine-grained soils is described. Databases consisting of static and cyclic triaxial test results, including maximum shear and post-cyclic volumetric strains, in conjunction with Atterberg limits, natural moisture content, applied static and cyclic shear stresses are used in the development of these correlations. For this purpose, series of static and cyclic triaxial tests were performed on isotropically and anisotropically consolidated undisturbed fine-grained samples. The results of these ongoing studies are summarized in the form of a semi-empirical stochastic model which enables the estimation of cyclically-induced volumetric and deviatoric straining as a function of liquid limit, plasticity index, natural moisture content, undrained shear strength, static and cyclic shear stresses.

Keywords: Fine-grained soils, cyclic triaxial tests, deviatoric strains, volumetric strains, maximum likelihood method

### INTRODUCTION

Over four decades have been passed since the pioneer studies performed on cyclic behavior of fine-grained soils. Initially, unlike loose saturated cohesionless soils, cohesive soils had been considered to be resistant to cyclic loading due to cohesion component of shear strength. For fine-grained soils potential problems under dynamic loading were generally associated to the degradation of its stiffness (Thiers and Seed (1968), Castro and Christian (1976), Idriss et al. (1978)). Increasing research interests were shown in understanding their cyclic response, after fine-grained soil ground failure case histories following 1975 Haicheng and 1979 Tangshan earthquakes in China. Chinese Criteria (Wang, 1979) have been proposed to assess liquefaction susceptibility of clayey soils and these criteria had been used widely with slight modifications (Seed et al. (1983), Finn et al. (1994), Perlea (1999)). More recently, ground failure case histories after 1989 Loma-Prieta, 1994, Northridge, and more importantly, 1999 Kocaeli and 1999 Chi-Chi earthquakes have accelerated studies on assessing cyclic mobility response of clayey soils as case histories from these earthquakes highlighted that low plasticity silt-clay mixtures might significantly strain-soften which may in turn cause significant damage to overlying structural systems. As an alternative to Chinese Criteria, based on field observations and laboratory cyclic test results Seed et al. (2003), Bray and Sancio (2006) and Boulanger and Idriss (2006) have recently recommended new criteria for the assessment of liquefaction triggering potential of fine-grained soils. Bray and Sancio (2006) have indicated that strength loss is significantly affected by the ratio ( $w_c / LL$ ). Whereas, as an alternative, Boulanger and Idriss (2006) have proposed liquidity index ( $LI$ ) term defined as the ratio of the difference ( $w_c - PL$ ) to  $PI$ . Additionally, Boulanger and Idriss (2004) have also presented a methodology to

---

<sup>1</sup> Research Assistant, Department of Civil Engineering, Middle East Technical University, Ankara, Turkey, Email: htbilge@metu.edu.tr.

<sup>2</sup> Associate Professor, Department of Civil Engineering, Middle East Technical University, Ankara, Turkey.

assess triggering of “cyclic failure” in clayey soils. As seen previous efforts have been confined to improve ability to assess identification of fine-grained soils susceptible to liquefaction. Meanwhile, on a separate stream, number of studies was performed aiming to determine the important factors affecting dynamic behavior of cohesive soils (Matsui et al. (1980), Kokusho et al. (1982), Andersen (1983), Ishihara (1986), Dobry and Vucetic (1987), Sun et al. (1988)). As nicely summarized in Vucetic and Dobry (1991), the most influential factor affecting dynamic behavior of cohesive soils was concluded to be plasticity index ( $PI$ ), and shear modulus degradation relationships were proposed as function of it.

As also illustrated by the presented literature, there exist a significant gap in the assessment of cyclically-induced deviatoric and volumetric (reconsolidation) straining of fine-grained soils. Previous studies mostly focused on sandy soils, due to significant cyclic straining potential of them. Some of these studies produced semi-empirical models for the assessment of cyclic straining in clean sands (e.g. Tokimatsu and Seed (1984), Ishihara and Yoshimine (1992), Shamoto et al. (1998)). On the other hand, only a few attempts can be listed for the estimation of cyclically-induced straining in fine-grained soils. Ohara and Matsuda (1988) and Yasuhara et al. (2001) have proposed new constitutive models founded on cyclic test results along with one-dimensional consolidation theory for the prediction of cyclically induced ground settlements in normally- or over-consolidated clayey soils. The former method was primarily based on the generation of excess pore water pressure due to applied uniform strain cycles. Inspired by the theory of one-dimensional consolidation, volumetric strains were estimated in terms of excess pore water pressure, initial void ratio and the compression index induced by cyclic loading. However, due to difficulties in the estimation of model input parameters, which require cyclic soil testing, the proposed method had a limited impact on practical applications. Similarly, Yasuhara et al. (2001) proposed an alternative methodology which enabled the assessment of both immediate and post-cyclic settlements. In this method, volumetric straining is expressed as a function of cyclically-induced excess pore water pressure, plasticity index and factor of safety against bearing capacity. Within the framework of one-dimensional consolidation theory, a constitutive model and as well as chart solutions were presented, which unfortunately require unpractical and time consuming, two- or three-dimensional dynamic numerical analyses for the determination of excess pore water pressure distribution within a soil media. As clearly presented, most studies have focused on volumetric straining and there was no existing work to our knowledge, regarding quantifying cyclically-induced shear straining in fine-grained soils.

Inspired by this gap, the aim of this study is defined as the development of a probabilistically-based semi-empirical, practical to use, model for the assessment of maximum shear and post-cyclic volumetric (reconsolidation) straining of saturated fine-grained soils subjected to 20 uniform loading cycles, corresponding to equivalent number of cycles a moment magnitude,  $M_w$ , 7.5 earthquake would produce (Liu et al., 2001). For this purpose, series of static and cyclic triaxial, as well as oedometer tests have been performed on undisturbed fine-grained soil samples. Details of the compilation and assessment efforts, as well as triaxial testing along with the presentation of the applied probabilistic framework, will be discussed in following sections.

## **TRIAXIAL TESTING PROGRAM AND EXPERIMENTAL RESULTS**

In this study, consolidated undrained strain-controlled static and stress-controlled cyclic triaxial tests have been performed on both isotropically- and anisotropically-consolidated undisturbed fine-grained soil samples. Oedometer tests were performed to understand the consolidation stress history of the samples. Besides, simple index tests were performed to determine Atterberg limits, specific gravity ( $G_s$ ), grain size distribution and natural moisture content of each sample. The undisturbed samples were taken mostly from Adapazari city. The liquid limit ( $LL$ ) and plasticity index ( $PI$ ) of the samples varied in the ranges of 25 to 60, and 4 to 34, respectively. For the resulting database, average values of  $LL$  and  $PI$  is 39 and 14, respectively. More than 85 % of the samples tested in this study are classified as either ML or CL, according to Unified Classification system. The ratio ( $w_c / LL$ ) was found to be in the range of 0.4 to 1.1 with the average value of 0.8.

## Static Triaxial Testing

Strain controlled static triaxial tests have been performed on 7.2 cm long triaxial test specimens with 3.6 cm in diameter, for the purpose of estimating their monotonic undrained shear strength,  $s_u$ . Consistent with ASTM D4767-88, the specimens were saturated by back-pressure until a B-value of minimum 0.96 is achieved. Samples were consolidated to a horizontal to vertical effective stresses ( $\sigma'_h / \sigma'_v$ ) varied in the range of 0.4 to 1.0, where the upper limit indicates isotropical consolidation. Horizontal effective consolidation stresses varied in the range of 60 to 150 kPa depending on the corresponding stress state in the field from which the undisturbed samples were taken. Following the saturation and consolidation phases, axial strain at a rate of 1%/min is applied until the sample fails. During monotonic straining of specimens; i) cell pressure, ii) pore water pressure, iii) axial deformation in specimen, and iv) axial load were recorded at every 2 seconds.

ASTM D4767-88 adopts different failure criteria depending on strain hardening or softening failure modes. For strain softening specimens, defining the peak undrained shear strength is rather trivial due to a well-defined peak deviatoric stress. However, for strain-hardening materials, usually samples with high silt contents in our case, definition of the peak deviatoric stress is not easy. Thus, for strain hardening samples, maximum stress obliquity,  $(\sigma'_1 / \sigma'_3)$ , criterion, consistent with the recommendations of ASTM D4767-88, was adopted.  $s_u$  values ranged from 30 to 220 kPa covering soft to stiff soil range. Each test has been carried until specimen exhibited a pronounced contractive or dilative response to enable the estimation of effective angle of friction ( $\phi'$ ).

A sample test result is presented in Figure 1 corresponding to a ML ( $LL = 31$  and  $PI = 6$ ) type specimen consolidated isotropically under an effective confinement pressure of 100 kPa. Peak deviatoric stress has been occurred at around 12 % axial strain, and estimated as 277 kPa. The maximum stress obliquity was observed at 5.5 % axial strain and corresponding deviatoric stress was determined as 205 kPa from stress-strain plot, and half of this value (103 kPa) was selected as the  $s_u$ . The last figure has shown the stress path followed during the testing. The initial contractive behavior was followed by a dilative behavior. From this figure, the peak effective angle of friction ( $\phi'$ ) was estimated as  $40^\circ$  which was interpreted as significantly higher than the typical values for clays. However, for clayey silt samples similar high values were also reported by Bray and Sancio (2006)

## Cyclic Triaxial Testing

Stress-controlled cyclic triaxial tests have been performed to assess cyclic straining behavior of fine-grained soil samples. Identical specimen saturation and consolidation stress stages were followed hoping to lead to identical samples tested under static and cyclic loads. In cyclic shearing stage, the deviatoric stresses were selected as a fraction of the undrained shear strength which had already been determined by static tests for the “identical” sample. The frequency of cyclic loading was selected as 1 Hz which is a common seismic loading rate. As previously stated by various researchers (e.g.: Zergoun and Vaid, 1994), for high frequency loading, it is unfortunately not possible to monitor the effective stress response of fine-grained soils due to delayed pore water pressure equalization. However, slower loading might cause other problems such as creep which may dominate straining in high plasticity soils (Zavoral and Campanella, 1994). 1 Hz loading was decided to be the optimum value to the solution of problems due to creep and keeping loading constant. Samples were subjected to 20 deviatoric loading cycles simulating the duration of an earthquake of moment magnitude 7.5. During cyclic shearing, i) cell pressure, ii) pore water pressure, iii) axial deformation in specimen and iv) applied axial load were recorded at 25 milliseconds. After 20<sup>th</sup> cycles, loading was stopped and samples were reconsolidated to the initial confining stress state, during which volumetric strain measurements were taken. Axial strain measurements were scaled by a factor of 1.5 to obtain shear strain values, consistent with the recommendation of Ishihara and Yoshimine (1992).

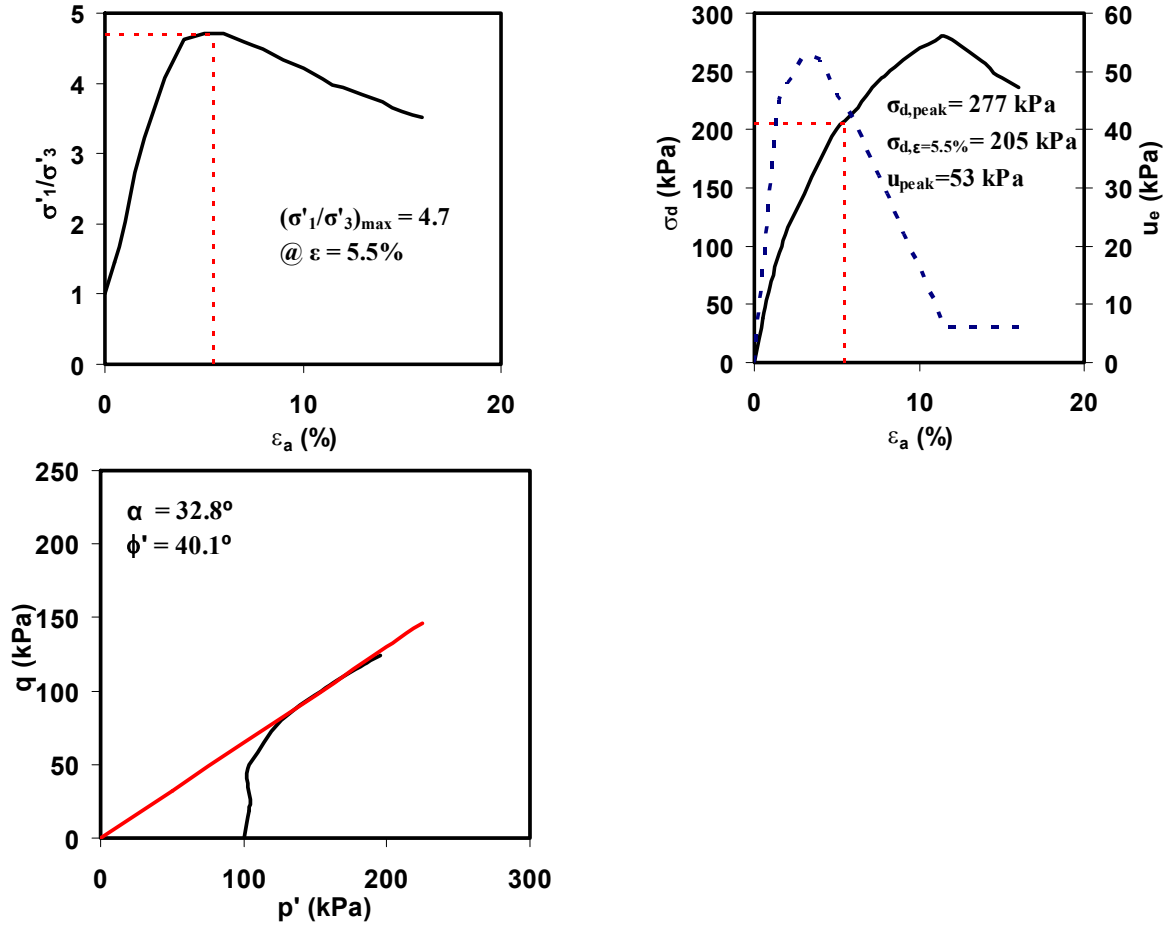


**Figure 1. A sample static triaxial test**

A sample presentation of cyclic test result is illustrated in Figure 2 for an ML type soil specimen with  $PI$  of 9. Its  $w_c / LL$  value was estimated as 0.9, fulfilling potentially liquefiable criteria of Seed et al. (2003) and Bray and Sancio (2006). The sample was consolidated isotropically under a confinement pressure of 110 kPa, and subjected to approximately 65 kPa of cyclic deviatoric stress in each loading cycle. In the presented four-way plots, cyclic response of the sample in the form of pore water pressure generation, shear strain accumulation as well as dilation and contraction transitions under cyclic shearing is illustrated. Load term,  $\tau_{cyc} / s_u$ , is expressed as the ratio of applied cyclic shear stress to undrained shear strength corresponding to the stress state sample was consolidated to. Maximum double amplitude cyclic shear strain is determined from the lower-right figure as 20.1 %.

For anisotropically consolidated specimens, static shear stress ( $\tau_{st}$ ) existed besides applied cyclic shear stress ( $\tau_{cyc}$ ). The ratio of static to cyclic shear stresses ranged from 0.0 to 2.0 where 0.0 has meant isotropical consolidation.

Table 1 summarizes the resulting database including the maximum double amplitude cyclic shear strain ( $\gamma_{max}$ ) and post-cyclic volumetric strain ( $\epsilon_v$ ) values recorded during and after 20 loading cycles, respectively. Atterberg limits, natural moisture content, effective vertical ( $\sigma'_{1,c}$ ) and horizontal ( $\sigma'_{3,c}$ ) consolidation stresses, and values of the ratio of applied static and cyclic shear stresses to undrained monotonic shear strength ( $s_u$ ) were also presented. It is also schematically shown in Figure 3. If the undrained shear strengths of samples are selected as the capacity term, then the ratio of  $\tau_{cyc} / s_u$  (x-

axes) and the ratio of  $\tau_{st} / s_u$  (y-axes) on Figure 3, indicate the percentage of capacity used during cyclic and static loading phases, respectively.

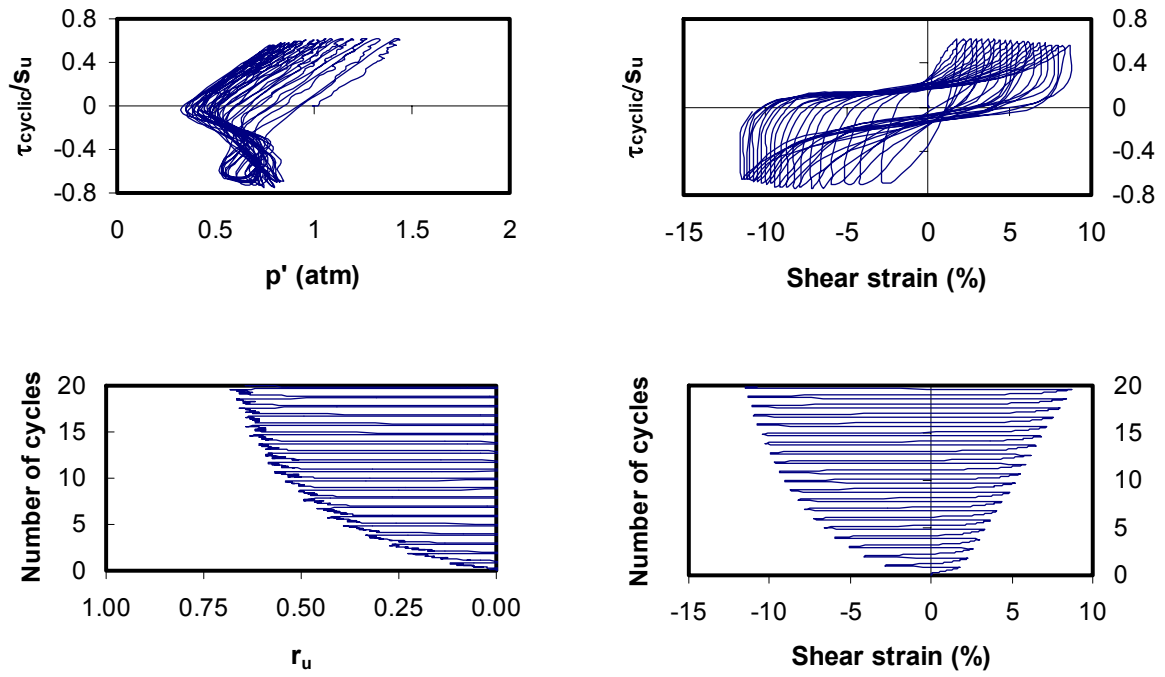


Figure 2. A sample cyclic triaxial test result

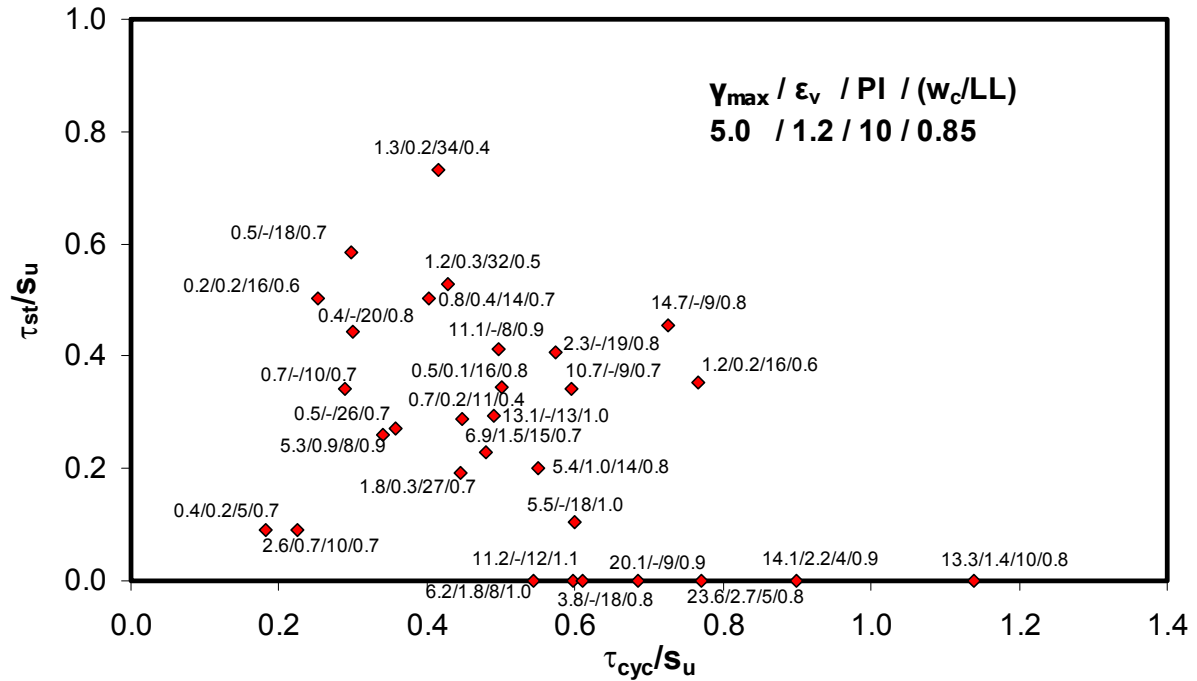


Figure 3. Cyclically-induced strain database used in this study

**Table 1. Summary of Cyclic Straining Database**

| Test No | LL | PL | PI  | w <sub>c</sub> (%) | w <sub>c</sub> /LL | σ' <sub>3,c</sub> (kPa) | σ' <sub>1,c</sub> (kPa) | s <sub>u</sub> (kPa) | τ <sub>cyc</sub> /s <sub>u</sub> | τ <sub>st</sub> /s <sub>u</sub> | r <sub>u</sub> | Y <sub>max,cyc</sub> (%) | ε <sub>vol</sub> (%) |
|---------|----|----|-----|--------------------|--------------------|-------------------------|-------------------------|----------------------|----------------------------------|---------------------------------|----------------|--------------------------|----------------------|
| 1       | 34 | 22 | 12  | 38.8               | 1.14               | 120                     | 120                     | 82                   | 0.60                             | 0.00                            | 0.23           | 11.2                     | NA                   |
| 2       | 39 | 21 | 18  | 39.1               | 1.00               | 100                     | 115                     | 72                   | 0.60                             | 0.10                            | 0.3            | 5.5                      | NA                   |
| 3       | 37 | 24 | 13  | 36.2               | 0.98               | 145                     | 212                     | 114                  | 0.49                             | 0.29                            | 0.65           | 13.1                     | NA                   |
| 4       | 50 | 24 | 26  | 36.9               | 0.74               | 120                     | 171                     | 94                   | 0.36                             | 0.27                            | 0.17           | 0.5                      | NA                   |
| 5       | 35 | 26 | 9   | 32.0               | 0.91               | 120                     | 120                     | 95                   | 0.68                             | 0.00                            | 0.68           | 20.1                     | NA                   |
| 6       | 44 | 25 | 19  | 36.5               | 0.83               | 120                     | 194                     | 91                   | 0.57                             | 0.41                            | 0.24           | 2.3                      | NA                   |
| 7       | 40 | 20 | 20  | 30.1               | 0.75               | 145                     | 245                     | 110                  | 0.30                             | 0.44                            | 0.03           | 0.4                      | NA                   |
| 8       | 41 | 23 | 18  | 30.6               | 0.75               | 147                     | 147                     | 95                   | 0.61                             | 0.00                            | 0.13           | 3.8                      | NA                   |
| 9       | 41 | 23 | 18  | 28.6               | 0.70               | 147                     | 343                     | 168                  | 0.30                             | 0.58                            | 0.06           | 0.5                      | NA                   |
| 10      | 35 | 26 | 9   | 28.4               | 0.81               | 93                      | 128                     | 73                   | 0.73                             | 0.45                            | 0.44           | 14.7                     | NA                   |
| 11      | 35 | 26 | 9   | 25.6               | 0.73               | 93                      | 162                     | 101                  | 0.60                             | 0.34                            | 0.55           | 10.7                     | NA                   |
| 12      | 32 | 24 | 8   | 29.7               | 0.93               | 93                      | 177                     | 102                  | 0.50                             | 0.41                            | 0.46           | 11.1                     | NA                   |
| 13      | 34 | 24 | 10  | 23.4               | 0.69               | 93                      | 211                     | 173                  | 0.29                             | 0.34                            | 0.43           | 0.7                      | NA                   |
| 14      | 31 | 21 | 10  | 23.2               | 0.75               | 100                     | 100                     | 40                   | 1.14                             | 0.00                            | 0.51           | 13.3                     | 1.4                  |
| 15      | 42 | 26 | 16  | 24.5               | 0.58               | 100                     | 129                     | 84                   | 0.77                             | 0.35                            | 0.11           | 1.2                      | 0.15                 |
| 16      | 36 | 28 | 8   | 31.4               | 0.87               | 100                     | 169                     | 133                  | 0.34                             | 0.26                            | 0.17           | 5.3                      | 0.92                 |
| 17      | 40 | 24 | 16  | 31.7               | 0.77               | 100                     | 169                     | 100                  | 0.50                             | 0.34                            | 0.05           | 0.5                      | 0.14                 |
| 18      | 40 | 26 | 14  | 32.0               | 0.80               | 100                     | 139                     | 100                  | 0.55                             | 0.20                            | 0.37           | 5.4                      | 1.04                 |
| 19      | 44 | 29 | 15  | 32.7               | 0.74               | 100                     | 139                     | 88                   | 0.48                             | 0.23                            | 0.58           | 6.9                      | 1.5                  |
| 20      | 27 | 16 | 11  | 11.5               | 0.42               | 100                     | 149                     | 85                   | 0.45                             | 0.29                            | 0.36           | 0.7                      | 0.2                  |
| 21      | 52 | 25 | 27  | 37.7               | 0.72               | 60                      | 94                      | 90                   | 0.44                             | 0.19                            | 0.12           | 1.8                      | 0.29                 |
| 22      | 30 | 22 | 8   | 28.5               | 0.95               | 100                     | 100                     | 70                   | 0.54                             | 0.00                            | 0.3            | 6.2                      | 1.8                  |
| 23      | 30 | 25 | 5   | 25.1               | 0.84               | 100                     | 100                     | 70                   | 0.77                             | 0.00                            | 1              | 23.6                     | 2.7                  |
| 24      | 40 | 24 | 16  | 24.6               | 0.62               | 100                     | 218                     | 119                  | 0.25                             | 0.50                            | 0.17           | 0.2                      | 0.15                 |
| 25      | 38 | 24 | 14  | 27.4               | 0.72               | 100                     | 218                     | 119                  | 0.40                             | 0.50                            | 0.2            | 0.8                      | 0.4                  |
| 26      | 34 | 25 | 9.5 | 24.1               | 0.70               | 100                     | 129                     | 165                  | 0.22                             | 0.09                            | 0.33           | 2.6                      | 0.7                  |
| 27      | 30 | 25 | 4.9 | 20.8               | 0.70               | 100                     | 129                     | 165                  | 0.18                             | 0.09                            | 0.17           | 0.4                      | 0.15                 |
| 28      | 60 | 26 | 34  | 24.7               | 0.41               | 100                     | 228                     | 82                   | 0.41                             | 0.73                            | 0.16           | 1.3                      | 0.15                 |
| 29      | 60 | 28 | 32  | 32.5               | 0.54               | 100                     | 179                     | 70                   | 0.43                             | 0.53                            | 0.24           | 1.2                      | 0.3                  |
| 30      | 25 | 21 | 4   | 23.3               | 0.93               | 100                     | 100                     | 30                   | 0.90                             | 0.00                            | 1              | 14.1                     | 2.21                 |

### Discussion of Experimental Results

Due to inevitable variability in controlling parameters, (i.e.:  $PI$ ,  $w_c / LL$ ,  $\tau_{cyc} / s_u$ ,  $\tau_{st} / s_u$ ) of natural soil samples, unfortunately interpretations of results were not easy compared to the ones of controlled tests where only one controlling factor is changed at a time. However, after studying Table 1 and Figure 3, carefully, following observations could be made.

- Consistent with previous findings in the literature, it is observed that  $PI$  is a controlling parameter for cyclic straining. As  $PI$  increases, resistance of material to cyclic stresses also increases and resulting strains decrease. Based upon our preliminary test results, beyond  $PI = 15$ , the cyclic straining are concluded to be limited ( $< 7.5$  %) for a cyclic shear stress ratio ( $\tau_{cyc} / s_u$ ) of 0.50.

- ii. The amplitude of  $\tau_{cyc} / s_u$  is important as it is the cyclic demand term. Below a threshold  $\tau_{cyc} / s_u$  value of 0.45, cyclic stresses can not accumulate significant shear strains (i.e. < 2.5 %).
- iii. The ratio of applied static stress to cyclic stress is important as it determines the occurrence of stress reversal. As indicated in previous studies (e.g.: Konrad and Wagg, 1993) presence of stress reversals may significantly increase cyclically-induced shear strains. Beyond a value of 0.6, the amplitude of cyclic shear strains is limited.
- iv. Last but not least, the ratio of soil samples' natural moisture content to its liquid limit ( $w_c / LL$ ) was found to be a significant parameter for the estimation of shear strain (or flow) potential of soils, consistent with the findings of recent, liquefaction triggering studies of Bray and Sancio (2006) and Boulanger and Idriss (2006). It was concluded that shear straining become smaller as  $w_c / LL$  decreases, and below a value of 0.7, no significant soil shear straining was observed.

Due to less number of post-cyclic volumetric strain data, it is difficult to make detailed observations. However, as illustrated in Figure 4, post-cyclic volumetric straining is strongly correlated to the maximum cyclic shear straining as also observed in cohesionless soil response (Ishihara and Yoshimine, 1992).

Despite limited number of available test results of this ongoing study, it is attempted to develop a probabilistic framework for the illustrative assessment of cyclic soil straining in fine-grained soils as it will be discussed next.

## DEVELOPMENT OF PROBABILISTIC MODELS FOR CYCLIC STRAIN PREDICTION

The first step in developing a probabilistic model is to select a limit state expression that captures the essential parameters of the problem. The model for the limit state function has the general form  $g = g(\mathbf{x}, \Theta)$  where  $\mathbf{x}$  is a set of descriptive parameters and  $\Theta$  is the set of unknown model parameters. Inspired by trends in the presented database, the following model is adopted as the limit state function for maximum cyclic double amplitude shear strain ( $\gamma_{max}$ ):

$$g_{\gamma_{max}}\left(\frac{w_c}{LL}, PI, \frac{\tau_{cyc}}{s_u}, \frac{\tau_{st}}{s_u}, \gamma_{max}, \Theta\right) = \ln(\gamma_{max}) - \ln\left[\theta_1 \cdot \frac{\theta_2\left(\theta_3, \frac{w_c}{LL}\right)}{\ln(PI)} \cdot \frac{\theta_4 - \sqrt{\left(\frac{\tau_{st}}{s_u} - \theta_5\right)^2 + \left(\frac{\tau_{cyc}}{s_u} - \theta_6\right)^2}}{\theta_4 - \theta_7}\right] \pm \varepsilon_{\gamma_{max}} \quad (1)$$

where  $\theta_i$  are the set of unknown model parameters.

The proposed model include a random model correction term ( $\varepsilon$ ) to account for the facts that i) possible missing descriptive parameters with influence on cyclic straining may exist; and ii) the adopted mathematical expression may not have the ideal functional form. It is reasonable and also convenient to assume that  $\varepsilon$  has normal distribution with zero mean for the aim of producing an unbiased model (i.e., one that in the average makes correct predictions). The standard deviation of  $\varepsilon$ , denoted as  $\sigma_\varepsilon$ , however is unknown and must be estimated. The set of unknown parameters of the model, therefore, is  $\Theta = (\theta, \sigma_\varepsilon)$ .

Assuming the maximum shear strain values of each cyclic shear test to be statistically independent, the likelihood function for “n” tests can be written as the product of possibilities of the observations, i.e.,

$$L_{\gamma_{max}}(\boldsymbol{\theta}, \sigma_{\varepsilon}) = \prod_{i=1}^n P \left[ g_{\gamma_{max}} \left( \frac{w_c}{LL_i}, PI_i, \frac{\tau_{st}}{s_{u_i}}, \frac{\tau_{cyc}}{s_{u_i}}, \varepsilon_{\gamma_{max},i}, \boldsymbol{\theta} \right) = 0 \right] \quad (2)$$

Suppose the values of  $(w_c / LL)_i$ ,  $PI_i$ ,  $(\tau_{st} / s_{u_i})_i$ , and  $(\tau_{cyc} / s_{u_i})_i$  at the each data point are exact, i.e. no measurement error is present, noting that  $g(\dots) = \hat{g}(\dots) + \varepsilon_i$  has the normal distribution with mean  $\hat{g}$  and standard deviation  $\sigma_{\varepsilon}$ , then the likelihood function can be written as:

$$L_{\gamma_{max}}(\boldsymbol{\theta}, \sigma_{\varepsilon}) = \prod_{i=1}^n \phi \left[ \frac{\hat{g}_{\gamma_{max}} \left( \frac{w_c}{LL_i}, PI_i, \frac{\tau_{st}}{s_{u_i}}, \frac{\tau_{cyc}}{s_{u_i}}, \boldsymbol{\theta} \right)}{\sigma_{\varepsilon_{\gamma_{max}}}} \right] \quad (3)$$

where  $\phi[\cdot]$  is the standard normal probability density function. Note that the above is a function of the unknown parameters. As part of maximum likelihood methodology, the coefficients which are estimated to maximize the likelihood functions given in Equation 3 are presented in Table 2. The maximum cyclic shear strain boundary curves for a representative case of  $PI = 8$  and  $w_c / LL = 0.9$  is presented in Figure 4 with compiled database. As there is not sufficient data at higher static and cyclic stress levels, some portions of the boundary curves are plotted by dashed lines. It should be noted that for each different  $PI$  and  $w_c / LL$  combination, a different set of curves could be developed by using Equation 1(or alternatively by Equation 5) along with the parameters summarized in Table 2.

As stated in previous section, there exists a correlation between post-cyclic volumetric and maximum cyclic shear strains. The maximum shear and post-cyclic volumetric strain pairs are presented in Figure 5. Simple regression analysis has been performed and following relation is obtained;

$$\varepsilon_v = -0.0047 \cdot \gamma_{max}^2 + 0.219 \cdot \gamma_{max} \quad (4)$$

**Table 2. Maximum Shear Strain Model Parameters**

|                        |       |
|------------------------|-------|
| $\theta_1$             | -1.07 |
| $\theta_2$             | 5.65  |
| $\theta_3$             | 1.80  |
| $\theta_4$             | 0.51  |
| $\theta_5$             | 0.41  |
| $\theta_6$             | -0.28 |
| $\theta_7$             | 0.10  |
| $\sigma_{\varepsilon}$ | 0.68  |



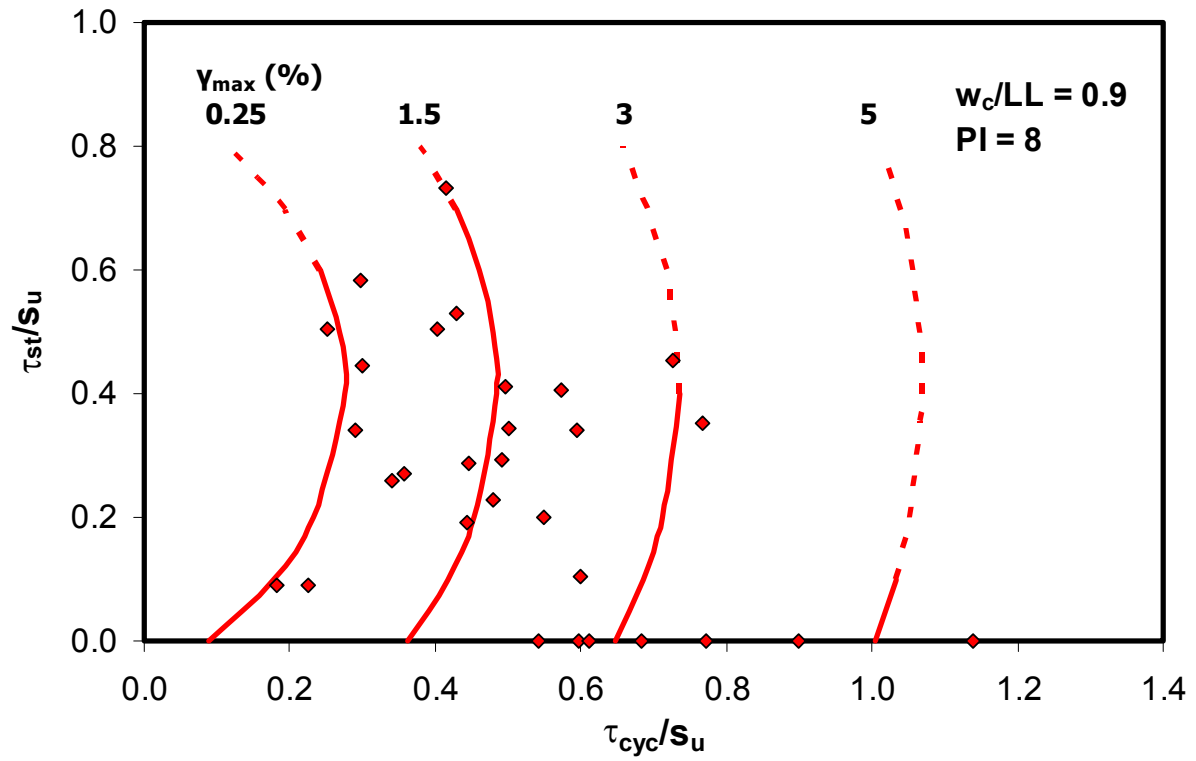


Figure 4. Maximum shear strain boundary curves

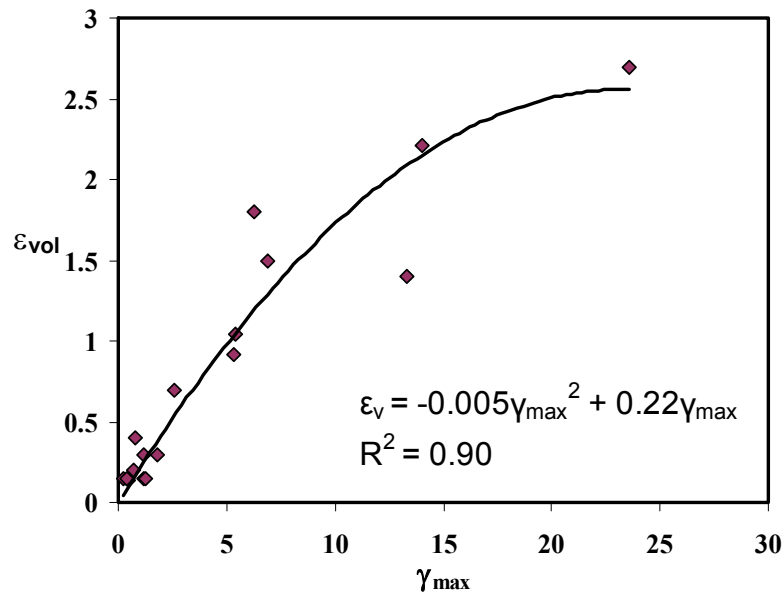


Figure 5. Relationship between  $\gamma_{\max}$  and  $\epsilon_v$

## SUMMARY AND CONCLUSIONS

Within the confines of this paper it is intended to develop a probabilistically- based semi-empirical model to predict cyclically induced maximum shear strains and post-cyclic volumetric strains in fine-grained soils. For this purpose, series of strain-controlled static and stress-controlled cyclic triaxial tests have been performed on undisturbed clayey samples and a database has been compiled. The important controlling parameters (descriptive variables) of the cyclic straining problem are found to be  $PI$ ,  $w_c / LL$ ,  $\tau_{cyc} / s_u$ , and  $\tau_{st} / s_u$ . The maximum likelihood methodology is used to develop

limit-state model incorporating these important descriptive variables for cyclically induced straining problem. The proposed model for maximum double amplitude shear straining is given in Equation 5. The predicted shear strains fall between 1:0.5 and 1:2 lines. The comparison of predicted and observed maximum shear strain values are presented in Figure 6. Proposed model yields slightly overestimated values in small strain range ( $\gamma_{max} < 2.5\%$ ), whereas for moderate to large strains ( $2.5 \leq \gamma_{max} \leq 15\%$ ) predictions are directly fall between boundaries. For large strain range ( $\gamma_{max} > 15\%$ ) proposed method slightly underestimates the measured values. However, in the overall the proposed model captured the general trend.

$$\ln(\gamma_{max}) = \ln \left( -1.07 \cdot \frac{5.65 \left( 1.80 \cdot \frac{w_c}{LL} \right)}{\ln(PI)} \cdot \frac{0.51 - \sqrt{\left( \frac{\tau_{st}}{s_u} - 0.41 \right)^2 + \left( \frac{\tau_{cyc}}{s_u} - (-0.28) \right)^2}}{0.51 - 0.10} \right) \pm 0.68 \quad (5)$$

Based on Equation 5, for constant  $\tau_{cyc} / s_u$  and  $\tau_{st} / s_u$  values it can be concluded that;

- If  $PI$  is doubled, resulting maximum cyclic shear strains may decrease approximately 30 % for constant  $w_c / LL$  ratio.
- If  $w_c / LL$  is doubled, resulting maximum cyclic shear strains may increase as much as 2.5 times, for constant  $PI$ .

In Figure 7, predicted and measured post-cyclic volumetric strains are compared based on maximum cyclic shear strain observations. A better match between predicted and observed values is obtained in all strain ranges as compared to shear strain predictions.

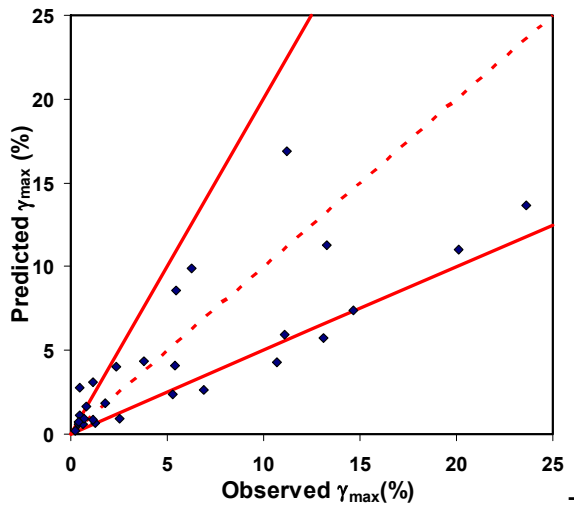


Figure 6. Comparison between observed and predicted maximum shear strains

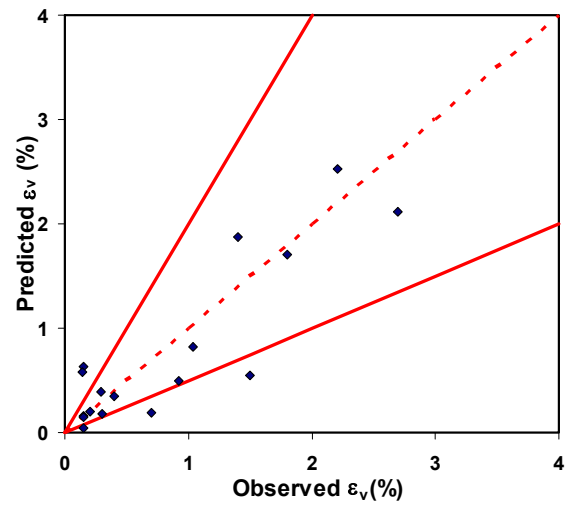


Figure 7. Comparison between observed and predicted post-cyclic volumetric strains

As the concluding remark, we would like to clarify our intention. All these preliminary findings were based on limited number of test results as part of our ongoing research studies. More samples are going to be tested at the i) plasticity ranges of ( $PI < 10$  and  $20 < PI < 60$ ), and ii) stress conditions corresponding to ( $\tau_{cyc} / s_u > 0.8$ ) and ( $\tau_{st} / s_u > 0.6$ ) where our current database has a gap. After these, we believe that the resulting model will be more general and powerful. However, even these limited

test results assessed within a probabilistic framework revealed that the proposed semi-empirical model is promising.

## ABBREVIATIONS

|                        |   |
|------------------------|---|
| $\varepsilon_a$        | Axial strain                                    |
| $\varepsilon_v$        | Post-cyclic volumetric (reconsolidation) strain |
| $\phi$                 | Peak angle of friction                          |
| $\gamma_{max}$         | Maximum double-amplitude cyclic shear strain    |
| $LL$                   | Liquid limit                                    |
| $LI$                   | Liquidity index                                 |
| $PI$                   | Plasticity index                                |
| $p'$                   | Mean effective stress                           |
| $r_u$                  | Excess pore water pressure ratio                |
| $s_u$                  | Undrained shear strength                        |
| $w_c$                  | Natural moisture content                        |
| $\sigma'_1, \sigma'_3$ | Major and minor principal stresses              |
| $\sigma_{dev}$         | Deviatoric stress                               |
| $\sigma'_h$            | Horizontal effective stress                     |
| $\sigma'_v$            | Vertical effective stress                       |
| $\tau_{cyc}$           | Cyclic shear stress                             |
| $\tau_{st}$            | Static Shear Stress                             |

## REFERENCES

- ASTM D4767-88 Standard Test Method for Consolidated-Undrained Triaxial Test on Cohesive Soils
- Boulanger RW and Idriss IM. "Liquefaction susceptibility criteria for silts and clays," Journal of Geotechnical and Geoenvironmental Engineering, ASCE, 1413-1426, 2006
- Boulanger RW and Idriss IM. "Evaluating the potential for liquefaction or cyclic failure of silts and clays," Rep. No. UCD/CGM-04/01, Center for Geotechnical Modeling, Dept. of Civil and Environmental Engineering, Univ. of California, Davis, Calif., 2004
- Andersen DG. "Strength and deformation properties of clay subjected to cyclic loading," Report No. 52412-8, Norwegian Geotechnical Institute, Oslo, Norway, 1983
- Bray JD and Sancio BS. "Assessment of the liquefaction susceptibility of fine-grained soils," Journal of Geotechnical and Geoenvironmental Engineering, ASCE, 1165-1177, 2006
- Castro G and Christian JT. "Shear strength of soils and cyclic loading," Journal of Geotechnical Engineering, ASCE, 887-894, 2006
- Dobry R and Vucetic M. "State-of-the-art report: Dynamic properties and response of soft clay deposits," Proc. International Symposium on Geotechnical Engineering of Soft Soils, Vol. 2, 51-87, 1987
- Idriss IM, Dobry R and Singh RD. "Nonlinear behavior of soft clays during cyclic loading," Journal of Geotechnical Engineering, ASCE, 1427-1447, 1978
- Ishihara K. "Evaluation of soil properties for use in earthquake response analysis," Geomechanical Modeling in Engineering Practice, Dingar R and Studer JA, eds., A. Balkema, Rotterdam, Netherlands, 241-275, 1986
- Ishihara K and Yoshimine M. "Evaluation of settlements in sand deposits following liquefaction during earthquakes," Soil Dynamics and Earthquake Engineering, 32, Issue 1, 861-878, 1992
- Kokusho T, Yoshida Y and Esashi Y. "Dynamic properties of soft clay for strain range," Soil Dynamics and Earthquake Engineering, 22, Issue 4, 1-18, 1982

- Liu H, Stewart JP, Abrahamson NA and Moriwaki Y. "Equivalent number of stress cycles for stress cycles for soil liquefaction analysis," *Journal of Geotechnical and Geoenvironmental Engineering*, ASCE, 1017-1026, 2001
- Matsui T, Ohara H and Ito T. "Cyclic stress-strain history and shear characteristics of clay," *Journal of Geotechnical Engineering*, ASCE, 1101-1120, 1980
- Ohara S and Matsuda H. "Study on the settlement of saturated clay layer induced by cyclic shear," *Soil Dynamics and Earthquake Engineering*, 28, Issue 3, 103-113, 1988
- Seed RB, Cetin KO, Moss RES, Kammerer A, Wu J, Pestana J, Riemer M, Sancio RB, Bray RE and Faris A. "Recent advances in soil liquefaction engineering: A unified and consistent framework," Keynote presentation, 26<sup>th</sup> Annual ASCE Los Angeles Geotechnical Spring Seminar, Long Beach, California, 2003
- Shamoto Y, Zhang J and Tokimatsu K. "New charts for predicting large residual post-liquefaction ground deformation," *Soil Dynamics and Earthquake Engineering*, 17, Issues 7-8, 427-438, 1998
- Sun JJ, Golesorkhi R and Seed HB. "Dynamic moduli and damping ratios for cohesive soils," Report No. EERC 88-15, Univ. of California, Berkeley, California, 1988
- Thiers GR and Seed HB. "Strength and stress-strain characteristics of clays subjected to seismic loading conditions," *Vibration Effects of Earthquakes on Soils and Foundations*, ASTM STP 450, American Society for Testing and Materials, 1968
- Tokimatsu K and Seed HB. "Simplified procedure for the evaluation of settlements in clean sands," Report No. UCB/EERC-84/16, Earthquake Engineering Research Center, College of Engineering, Univ. of California, Berkeley, California, 1984
- Vucetic M and Dobry R. "Effect of soil plasticity on cyclic response," *Journal of Geotechnical Engineering*, ASCE, 89-107, 1991
- Wang W. "Some findings in soil liquefaction engineering," *Water Conservancy and Hydroelectric Power Scientific Research Institute*, Beijing, China, 1979
- Yasuhara K, Murakami S, Toyota N and Hyde AFL. "Settlements in fine-grained soils under cyclic loading," *Soil Dynamics and Earthquake Engineering*, 41, Issues 6, 25-36, 2001
- Zavoral DZ and Campanella RG. "Frequency effects on damping modulus of cohesive soil," *Dynamic Geotechnical Testing II*, ASTM STP 1213, Ebelhar RJ, Drnevich VP and Kutter BL., eds., American Society for Testing and Materials, Philadelphia, 1994
- Zergoun M and Vaid YP. "Effective stress response of clay to undrained cyclic loading," *Canadian Geotechnical Journal*, 31, 714-727, 1994